Newly designed measurement system for the radon progeny activity size distribution based on screen diffusion battery

Hao Wang [a,b], Jinmin Yang [b], Changhao Sun [b,c], Lei Zhang [b,*], Qiuju Guo [a]

[a] State Key Laboratory of Nuclear Physics and Technology, School of Physics, Peking University, Beijing, 100871, China
[b] State Key Laboratory of NBC Protection for Civilian, Beijing, 102205, China
[c] Division of Ionizing Radiation Metrology, National Institute of Metrology, Beijing, 100029, China

ARTICLE INFO

ABSTRACT

Accurate measurement of the activity size distribution of radon progeny is of importance for dose evaluation. To meet the increasing demand for field survey in China, a new measurement system consisting of 8 stages wire screen diffusion battery was developed, by which the unattached fraction, the fraction of particles larger than 2.5 μm, the activity size distribution and the activity concentration of each radon progeny could be measured simultaneously. To verify the activity size distribution measurement results of the new measurement system, a series of comparison experiments were carried out with an indirect measurement method in radon chamber and indoor environment. The results in radon chamber exhibited a good consistency between the two methods in activity size ranging from 73 nm to 297 nm with an average deviation of −1%, but the result measured by the new system was smaller at 551 nm due to the loss of large particles during the sampling process. Comparison results in indoors mostly showed a good agreement as the deviations were less than 10%, and some large deviations were also observed, which was mainly on account of the limitation of sensitivity and measurement uncertainty.

1. Introduction

Radon and its short short-lived progeny are the greatest contributor of the natural radiation to human exposure (UNSCEAR, 2019). As reported by ICRP 137 (ICRP, 2017), the effective dose per unit exposure to radon progeny is strongly dependent on the particle size of the radon progeny and the unattached fraction. The size distribution of radon progeny is the second biggest contributing factors to effective dose, as pointed out by UNSCEAR (2019). Accurate measurement of the activity size distribution is therefore important and necessary for dose evaluation of radon exposure.

In China, few studies focusing on the field survey of radon progeny size distribution have been conducted, almost all based on the indirect method (Yamada et al., 2006; Zhang et al., 2010). With the increasing demand for field survey, a new direct measurement system is required.

For the purpose of field survey and independent measurement of radon progeny existing in different modes, a new measurement system based on screen diffusion battery was developed. To verify the measurement results of this new system, a series of comparison experiments were carried out in both radon chamber and indoor environment.

2. Materials and methods

2.1. Measurement system

The newly designed measurement system consists of eight parallel sampling and measurement subsystem with 55 cm × 55 cm × 45 cm in size and nearly 15 kg in weight, making it portable for field measurement. The schematic diagram and the picture are shown in Fig. 1, each parallel subsystem contained its own particle sampler, electronic unit, pump and flow meter. For Stage 1, all aerosols were collected onto a 0.45 μm PTFE filter (Haichengshijie, China) with nearly 100% collection efficiency. For stage 2 to stage 8, the HP2540 impactors (BGI, American) were deployed to separate the particles larger than 2.5 μm with the flowrate of 4 lpm. Different set of wire screen were mounted at stage 3 to stage 8 to absorb the unattached radon progeny and partially absorb the attached radon progeny (less than 2.5 μm) of different particle size. The rest aerosols penetrated through the impactor and wire screen and then were collected onto the filter.

The effective sampling areas of screens were 3.7 cm in diameter. According to the penetration characteristic of the PM2.5 impactor, the
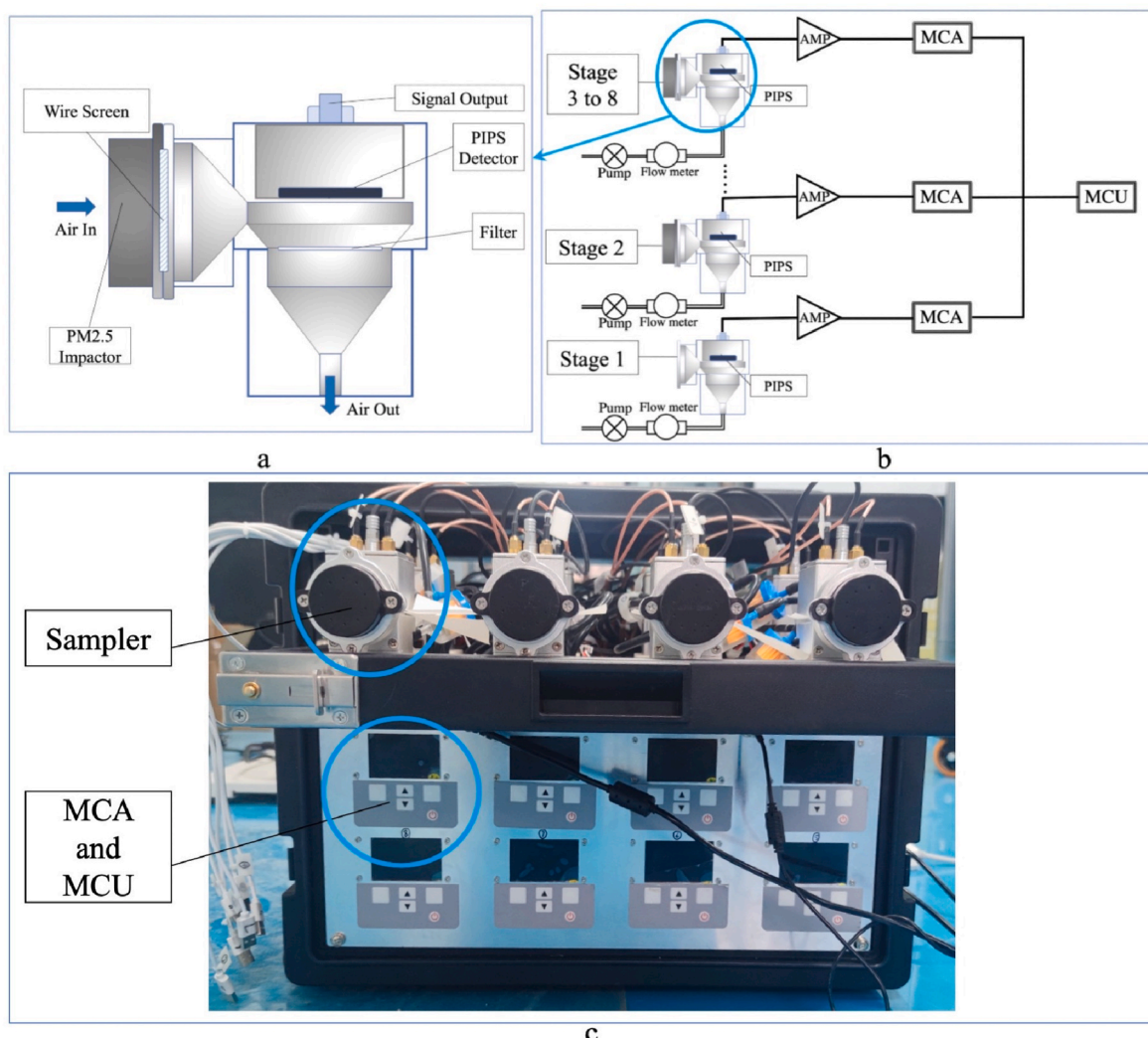

Fig. 1. The schematic diagram for the sampler **a)** and the measurement system **b)**. The picture of the measurement system **c)**.

Table 1
The diffusion battery parameters and the particle penetration of our system.

Stage	Mesh No.	Number of screen	Wire diameter d_f (μm)	Thickness L (mm)	Solid volume fraction	Penetration fraction
2	/	/	/	/		100%
3	135	1	60.0 ± 3.0	0.145 ± 0.001	0.208	98%
4	200	12	48.3 ± 2.4	0.140 ± 0.001	0.204	88%
5	400	18	29.8 ± 1.5	0.078 ± 0.001	0.318	79%
6	450	29	25.8 ± 1.3	0.058 ± 0.001	0.345	69%
7	500	45	22.1 ± 1.0	0.050 ± 0.001	0.366	59%
8	635	64	16.8 ± 1.0	0.039 ± 0.001	0.328	49%

sampling flowrate of each stage was stably controlled at 4 lpm, in which the PM2.5 impactor had a cut-off diameter of 2.5 μm. During sampling, the radon progeny activity collected on downstream filters were measured simultaneously by the 600 mm² Passivated Implanted Silicon (PIPS) detectors (AP-CAM28, Chengdu Jingwei Science And Technology Co Ltd.) and Multi-Channel Analyser (MCA). The detection efficiencies of eight detectors were calibrated to be from 23% to 25% by an electroplated ^{241}Am alpha source, which had been calibrated through intercomparison at National Institute of Metrology (NIM) of China. The alpha spectrum was recorded and analysed by Micro-Controller Unit (MCU). The counts of ^{218}Po and ^{214}Po could be calculated through the alpha spectrum.

The activity concentrations of ^{218}Po, ^{214}Pb, ^{214}Bi and Equilibrium Equivalent Concentration (EEC) were calculated using the optimized Wicke method (Yunxiang et al., 2021). The continuous measurement mode in which the sampling time synchronized with the measurement interval of 60 min following the gross alpha method (Kusnetz and Howard, 1956; Sakoda et al., 2020) was also used for low radon concentration environment, which based on the assumption that EEC is proportional to the gross alpha counts of radon progeny. and the EEC could be calculated by Eq. (1).

$$EEC = \varepsilon_\alpha^{-1} \bullet F^{-1} \bullet \varepsilon_f^{-1} \bullet K \bullet (N_1 + N_1 - 0.56N_3) \tag{1}$$

where ε_α is the alpha detection efficiency of the PIPS detector and the difference between the detection efficiency for different alpha particles was ignored here, F is the sampling flowrate (lpm), ε_f is the collection

Table 2
Comparison results of SDB direct method and the reference SMPS indirect method in radon chamber.

No	EEC (Bq/m³)	SMPS Calculated AMD (nm)	GSD	8-Stage SDB EEC (EM) AMD (nm)	GSD	EEC (TM) AMD (nm)	GSD	8-Stage SDB ^{218}Po (EM) AMD (nm)	GSD	^{218}Po(TM) AMD (nm)	GSD	8-Stage SDB ^{214}Pb (EM) AMD (nm)	GSD	^{214}Pb (TM) AMD (nm)	GSD	8-Stage SDB ^{214}Bi (EM) AMD (nm)	GSD	^{214}Bi (TM) AMD (nm)	GSD
1	384.8	81	1.7	79	1.5	75	1.9	71	1.6	76	1.6	77	1.6	74	1.6	76	1.5	76	1.7
2	250.4	73	1.7	65	1.5	61	1.9	64	1.5	68	1.5	49	1.6	51	1.6	75	1.2	75	1.2
3	419.3	83	1.7	82	1.5	80	1.9	79	1.4	79	1.4	82	1.5	101	1.5	82	1.6	79	1.6
4	741.7	119	1.3	121	1.3	116	1.4	142	1.3	135	1.3	122	1.3	113	1.3	116	1.3	107	1.5
5	466.0	125	1.3	123	1.4	127	1.3	119	1.4	129	1.4	119	1.4	125	1.4	140	1.4	141	1.2
6	1629.1	166	1.2	175	1.3	167	1.2	189	1.3	180	1.3	212	1.2	206	1.2	159	1.2	151	1.4
7	3886.3	166	1.2	164	1.2	169	1.2	152	1.3	166	1.3	169	1.2	166	1.2	162	1.2	175	1.2
8	2846.0	234	1.2	231	1.2	243	1.2	213	1.3	228	1.3	240	1.2	238	1.2	217	1.3	260	1.2
9	2473.1	266	1.2	279	1.2	265	1.2	327	1.3	338	1.1	289	1.1	302	1.1	275	1.2	273	1.4
10	2660.7	297	1.2	322	1.2	295	1.3	308	1.2	363	1.1	318	1.2	311	1.2	291	1.2	296	1.1
11	2386.5	551	1.1	394	1.2	403	1.2	345	1.4	352	1.1	338	1.1	343	1.1	329	1.2	333	1.1

efficiency of the filter. K is the calibration factor (($Bq \cdot lpm$)/($m^3 \cdot cph$)), which was calibrated through comparison in radon chamber. N_1, N_2 and N_3 are the alpha count rates of ^{218}Po (6.05 MeV), ^{214}Po (7.69 MeV) and ^{212}Po (8.78 MeV) in the 60 min measurement cycle (cph), separately.

2.2. Activity size distribution inversion

The activity size distribution can be approximately described by a sum of log-normal distributions in different environment (Porstendörfer et al., 2000). For the unimodal distribution environment, the size distribution can be simply described by a frequency function of the log-normal distribution with Activity Median Diameter (AMD) and the Geometric Standard Deviation (GSD, σ_g):

$$f\left(\ln d_p\right) = \frac{1}{\sqrt{2\pi} \cdot \ln \sigma_g} \cdot \exp\left(-\frac{\left(\ln d_p - \ln \text{AMD}\right)^2}{2\left(\ln \sigma_g\right)^2}\right) \tag{2}$$

The relation between the activity-weighted size distribution $f(d_p)$ and the measured activity concentration value μ_i in stage i is:

$$\mu_i = \int_0^\infty k\left(d_p\right) f\left(d_p\right) \mathrm{d}d_p + \varepsilon_i \tag{3}$$

where ε_i is the measurement error, $k(d_p)$ is the kernel function of the system and depends on the wire screens characteristics. In order to estimate the activity-weighted size distribution of radon progeny, both the Twomey algorithm (Twomey, 1975) and the Expectation Maximization algorithm (Maher and Laird, 1985) were applied to inverse the measured activity concentrations.

2.3. Comparison experiments

To confirm the measurement results of the system, comparison experiments were carried out in a radon chamber and indoor environment with the indirect measurement method as a reference. For the indirect method, a Scanning Mobility Particle Sizer (SMPS-5416, Grimm, Germany) was used to measure the number size distribution $Z(d_p)$, and then the activity-weighted size distribution $f(d_p)$ can be calculated using the following equations (Porstendorfer and Reineking, 1992; Jacobi, 1971):

$$\frac{f\left(d_p\right)}{C} = \frac{\beta\left(d_p\right) Z\left(d_p\right)}{\int_0^\infty \beta\left(d_p\right) Z\left(d_p\right) \mathrm{d}d_p} \tag{4}$$

$$\beta\left(d_p\right) = \frac{2\pi D_0 d_p}{\frac{8D_0}{v_0 d_p} + \frac{d_p}{2l_0 + d_p}} \tag{5}$$

where d_p is the particle diameter (nm), $\beta(d_p)$ is the attachment coefficient (m^3/s) of the particle diameter d_p, C is the attached radon progeny concentration (Bq/m^3), $D_0 = 6.8 \times 10^{-2}$ cm²/s is the diffusion coefficient, $v_0 = 1.72 \times 10^4$ cm/s is the mean thermal velocity, $l_0 = 4.9 \times 10^{-6}$ cm is the mean free path of the unattached progeny.

The radon chamber has 18 m^3 effective volume with the radon concentration, temperature and humidity automatically controlled. And the size of aerosols inside was adjusted by using a SLG-270 condensation monodisperse aerosol generator (Grimm, Germany). In total 11 groups of comparison experiments were carried out in radon chamber and 18 groups of comparison experiments were carried out in a real office room, EEC was measured with 60 min measurement cycle, while temperature and humidity were recorded.
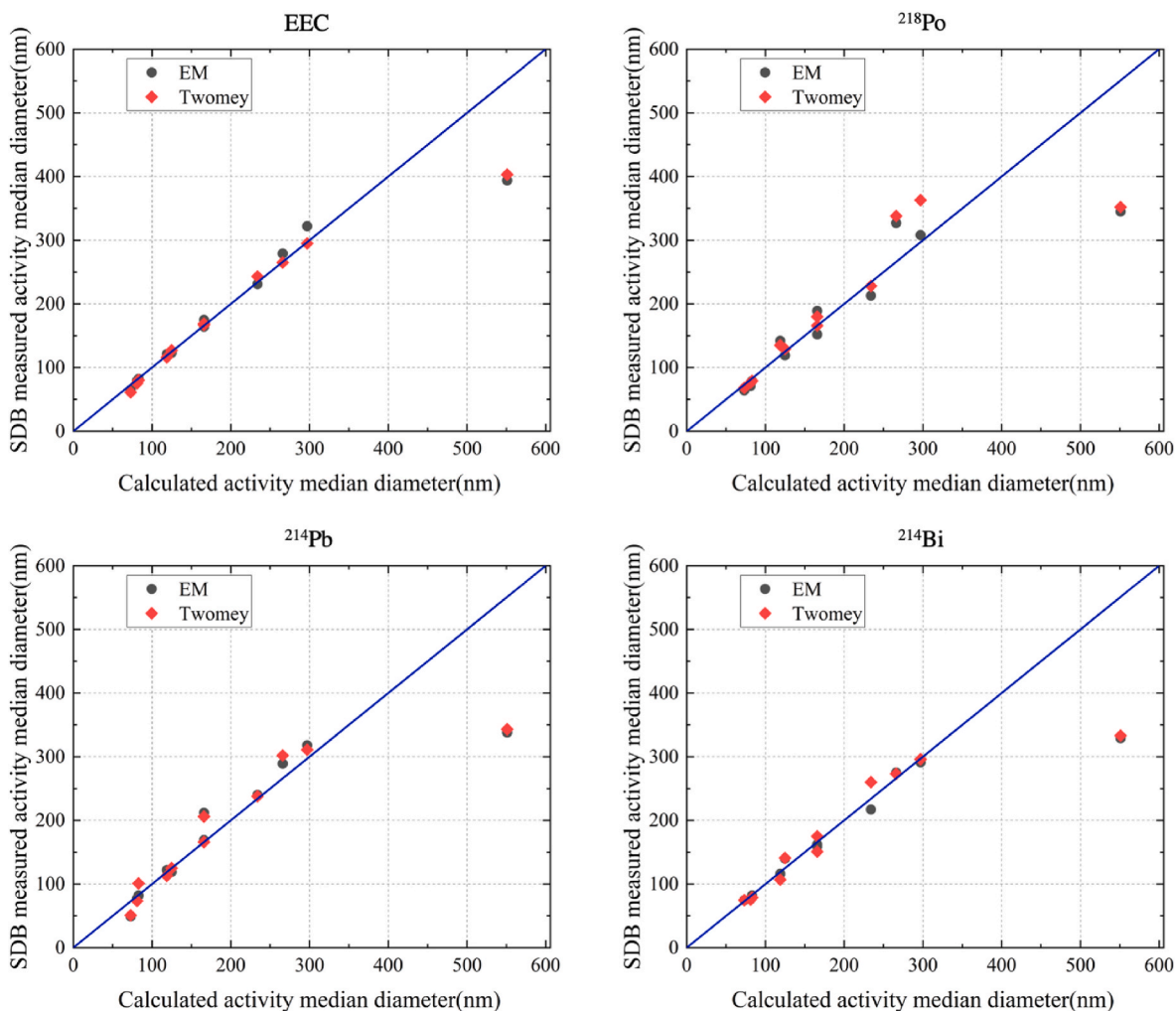
Fig. 2. Comparison of the AMD of EEC, ^{218}Po, ^{214}Pb and ^{214}Bi obtained by the SDB system with EM and Twomey algorithm, and the AMD derived from SMPS system in radon chamber.

Table 3
Comparison results of SDB direct method and the reference SMPS indirect method in indoors.

| No	EEC (Bq/m^3)	SMPS		8-Stage SDB					
		Calculated		EEC (EM)			EEC (TM)		
		AMD (nm)	GSD	AMD (nm)	Deviation (%)	GSD	AMD (nm)	Deviation (%)	GSD
1	29.6	186	1.8	191	2.7%	2.2	228	23%	2.1
2	37.2	204	1.8	200	−2.2%	2.1	187	−8.5%	2.0
3	30.3	222	1.7	221	−0.3%	2.3	229	3.3%	2.0
4	30.2	210	1.7	193	−8.1%	2.6	210	0.0%	2.1
5	6.3	205	1.8	214	4.4%	1.7	200	−2.4%	1.3
6	7.5	186	1.8	193	3.8%	1.5	217	17%	1.3
7	13.2	191	1.8	181	−5.1%	2.4	171	−10%	1.2
8	12.4	182	1.8	184	1.0%	1.8	186	2.1%	1.3
9	14.1	211	1.9	220	4.4%	1.4	217	3.0%	1.4
10	13.0	206	1.8	193	−6.4%	2.0	196	−4.9%	1.2
11	49.6	214	1.8	218	1.9%	1.9	219	2.3%	1.4
12	10.0	155	1.8	140	−9.9%	2.0	148	−4.7%	2.0
13	9.3	168	1.8	151	−10%	2.0	155	−7.6%	1.3
14	15.6	167	1.9	121	−28%	2.0	116	−31%	2.0
15	10.8	180	1.7	177	−1.9%	2.0	177	−1.9%	1.4
16	12.1	175	1.8	210	20%	2.0	206	18%	1.3
17	49.7	201	1.7	213	2.0%	2.0	210	0.5%	1.8
18	54.5	220	1.7	225	2.2%	2.1	211	−4.2%	1.6
Average	22.5	194	/	191	−1.6%	/	194	−0.4%	/
Range	6.3–54.5	155–222	1.7–1.9	121–225	/	1.4–2.6	116–229	/	1.2–2.1
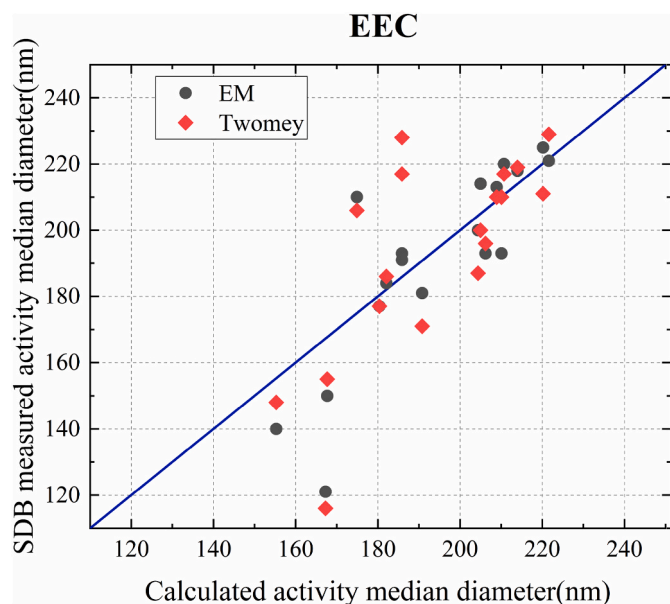
Fig. 3. Comparison of the AMD of EEC obtained by the SDB system with EM and Twomey algorithm, and the AMD derived from SMPS system in indoor environments.

3. Results and discussion

3.1. Optimized wire screen diffusion battery

For optimizing the wire screen selection, the penetration fraction of wire screens at typical indoor particle size bimodal distribution (activity median diameter of 30 nm and 250 nm, the same geometric standard deviation of 2.0 and a distribution ratio of 0.2:0.8)(ICRP Publication 137, 2017) were calculated using the fan filtration penetration theory (Cheng and Yeh, 1980). By adjusting the type and number of screens, the fraction of particles deposited on each stage changes almost linearly with the stages according to the theoretical calculation. The parameters and the penetration of the selected wire screens in stage 2 to stage 8 were shown in Table 1, The optimized wire screen diffusion battery was selected as 135 mesh × 1, 200 mesh × 12, 400 mesh × 18, 450 mesh × 29, 500 mesh × 45, 635 mesh × 64. Actually, the optimized selection of wire screen might be slightly different for different environment, but it is sufficient for real indoor environment survey.

3.2. Comparison results in radon chamber

The comparison experiment in radon chamber was conducted under 11 different aerosol conditions in the size range from 73 nm to 551 nm, and GSD ranged from 1.1 to 1.7. The EEC ranged from 250.4 to 3886.3 Bq/m^3. The temperature and relative humidity were set at 20 °C and 40%RH, respectively.

Comparison results are shown in Table 2. The calculated activity size distribution measured by SMPS system and the measured activity size distribution of EEC and ^{218}Po, ^{214}Pb and ^{214}Bi by the 8-stage SDB system with two inversion algorithms were listed.

For the direct measurement results of SDB system, there was no difference between the two inversion algorithms. The deviations between the two inversion algorithms were all within ±8% except for 3 of the 44 results (18% for ^{218}Po in No.10, 23% for ^{214}Pb in No.3, 20% for ^{214}Bi in No.8).

The comparison results of SDB system and indirect method at different particle size were shown in Fig. 2. Taking the AMD of EEC results for example, the deviations between the two methods were within −16% to 8% in activity size range from 73 nm to 297 nm, and the

average deviation is −1%. The small deviations corroborated a good consistency between the direct method and the indirect method. For the particle size of 551 nm, the particle size of EEC and ^{218}Po, ^{214}Pb and ^{214}Bi measured by SDB system were all smaller than the indirect method with average deviation of −36%. This size is close to the inflection point (maximum point) of the penetration-diameter curve of the wire screens, which means the penetration changes slightly with the particle diameter change. It is hard for the inversion algorithm to obtain the accurate value of particle size. In addition, the particle-laden air stream lines are curved, this can cause the larger particles of sufficient inertia to escape while the smaller particles with less inertia will follow the air stream lines and be collected on the filters.

No obvious difference in the activity size distribution of the ^{218}Po, ^{214}Pb, ^{214}Bi and EEC was observed in radon chamber environment. Taking the AMD of EEC as reference, the deviations of AMD of ^{218}Po, ^{214}Pb and ^{214}Bi were all within ±22% for the 11 groups of results, and the average deviation were 3%, 1%, −1%, respectively.

3.3. Comparison results in indoor environments

Comparison results in indoors are shown in Table .3 and Fig. 3. The EEC in indoor environment ranged from 6.3 to 54.5 Bq/m^3. All results were presented in a unimodal distribution, the AMD of EEC ranged from 155 nm to 222 nm with an average size of 194 nm, the GSD ranged from 1.7 to 1.9. For 14 groups of results, the deviations were less than 10%. Some large deviations were observed in experiment No1, 6, 14 and 16, which were 23%, 17%, −31% and 20%, respectively. The large deviations may be caused by the statistical uncertainty at the low EEC level and the error of inversion algorithm.

4. Conclusion

For field survey on the activity size distribution of radon progeny, a new measurement system based on screen diffusion battery was developed. Comparison experiments were carried out in both radon chamber and indoor environment with indirect measurement method. The results in radon chamber exhibited a good consistency between the two methods in activity size range from 73 nm to 297 nm, but the result measured by the new system was smaller at 551 nm. Comparison results in indoors mostly showed a good agreement in activity size range from 155 nm to 222 nm, while some large deviations were observed mainly due to the limitation of sensitivity. Results show that the new-designed system can give accurate activity size distribution in a wide range of aerosol size distribution making the new system be suitable for field measurement. More field survey results will be given in the future.

Declaration of competing interest

The authors declare that they have no known competing financial interests or personal relationships that could have appeared to influence the work reported in this paper.

Data availability

The data that has been used is confidential.

References

BGI Inc. HP2540 impactors. http://www.bgiusa.com.

Chengdu Jingwei Science And Technology Co Ltd. AP-CAM28 PIPS detector. http://www.techjw.com.

Cheng, Y.S., Yeh, H.C., 1980. Theory of a screen-type diffusion battery. J. Aerosol Sci. 11 (3), 313–320. https://doi.org/10.1016/0021-8502(80)90105-6.

GRIMM Aerosol Technik GmbH&Co.KG. SMPS-5416 scanning mobility particle sizer. www.grimm-aerosol.com.

, GRIMM Aerosol Technik GmbH&Co.KG. SLG-270 condensation monodisperse aerosol generator. www.grimm-aerosol.com.

Haichengshijie Filter Equipment Co Ltd. PTFE filter. http://www.hcsjgl.com/show.asp?id=65.

International Commission on Radiological Protection (ICRP), 2017. Occupational intakes of radionuclides: Part 3. ICRP Publication 137. Ann. ICRP 46 (3/4). https://doi.org/10.1177/0146645317734963.

Jacobi, W., 1971. Activity and potential energy of 222radon and 220radon-daughters in different air atmospheres. Health Phys. 22, 441–450. https://doi.org/10.1097/00004032-197205000-00002.

Kusnetz, M.S., Howard, L., 1956. Radon daughters in mine atmospheres a field method for determining concentrations. Am. Ind. Hyg. Assoc. J. 17 (1), 85–88. https://doi.org/10.1080/00968205609344380.

Maher, E.F., Laird, N.M., 1985. EM algorithm re-construction of particle size distributions from diffusion battery data. J. Aerosol Sci. 16, 557–570. https://doi.org/10.1016/0021-8502(85)90007-2.

Porstendorfer, J., Reineking, A., 1992. Indoor behaviour and characteristics of radon progeny. Radiat. Protect. Dosim. 45 (1–4), 303–311. https://doi.org/10.1093/rpd/45.1-4.303.

Porstendörfer, J., Zock, C., Reineking, A., 2000. Aerosol size distribution of the radon progeny in outdoor air. J. Environ. Radioact. 51 (1), 37–48. https://doi.org/10.1016/S0265-931X(00)00043-6.

Sakoda, A., Ishimori, Y., Kanzaki, N., Tanaka, H., 2020. Methodology for simple spot measurement of equilibrium equivalent radon concentration. Prot. Dosim. 191 (4) https://doi.org/10.1093/rpd/ncaa176.

Twomey, S., 1975. Comparison of constrained linear in- version and an iterative nonlinear algorithm applied to the indirect estimation of particle size distributions. J. Comput. Phys. 18, 188–200. https://doi.org/10.1016/0021-9991(75)90028-5.

United Nations Scientific Committee on the Effects of Atomic Radiation (UNSCEAR), 2019. Report: Sources and Effects of Ionizing Radiation, vol. 2021. United Nations Publications, ISBN 978-92-1-139184-8.

Yamada, Y., Sun, Q., Tokonami, S., et al., 2006. Radon–Thoron discriminative measurements in gansu province, China, and their implication for dose estimates. J. Toxicol. Environ. Health A 69, 723–734. https://doi.org/10.1080/15287390500261265.

Yunxiang, Wang, Changhao, Sun, Lei, Zhang, Qiuju, Guo, 2021. Optimized method for individual radon progeny measurement based on alpha spectrometry following the wicke method. March Radiat. Meas. 142, 106558. https://doi.org/10.1016/j.radmeas.2021.106558.

Zhang, L., Guo, Q., Zhuo, W., 2010. Measurement of the 212Pb particle size distribution indoors. Radiat. Protect. Dosim. 141, 371–373. https://doi.org/10.1093/rpd/ncq227.